DOI: 10.1002/cphc.201100246

Linking Spectral and Electrochemical Analysis to Monitor *c*-type Cytochrome Redox Status in Living *Geobacter sulfurreducens* Biofilms

Ying Liu,[a] Hoseang Kim,[b] Rhonda R. Franklin,[b] and Daniel R. Bond*[a]

When transferring electrons to insoluble Fe^{III} oxyhydroxide particles, the bacterium *Geobacter sulfurreducens* must utilize a chain of redox proteins to relay electrons from cytoplasmic electron carriers to external electron acceptors. In the presence of an electrode poised at an oxidizing potential, not only can cells in contact with the electrode respire directly to the surface, but 10 to 20 cell layers can stack upon each other, and each layer is also electrically connected to the electrode.[1–3] Thus, *G. sulfurrueducens* naturally self-assembles a three-dimensional network of proteins capable of oxidizing complex fuels, relaying electrons out of the cytoplasm and across their membranes, and through a biofilm as thick as 40 μm, to sustain current densities on the order of 1 mA cm^{-2}.[4,5] Such rates of simultaneous enzymatic oxidation and long-range current transfer rival those achieved by pure enzymes embedded in advanced redox hydrogels.[6]

The adaptation of electrochemical techniques to study and control this complex microbial electron-transfer process has opened a window into the physiology of these bacteria.[1,2,5,7–9] However, challenges remain in correlating voltammetry data with specific proteins, and understanding the molecular mechanism of long-distance electron relay between living cells.[10–13] Mutant analyses, immunogold labeling, and proteomic studies[7,14–18] have suggested roles for many different multiheme *c*-type cytochromes, as well as pili and multicopper proteins,[7,14,16,18–24] but less is known about their kinetics or activity in vivo.

The use of spectroscopic methods during potentiometric analysis of redox enzymes offers a tool to directly measure the redox status of multiple cofactors. When proteins are immobilized on transparent conductive electrodes, potential-dependent changes can be linked to specific redox centers.[25,26] Two recent reports extended spectral and electrochemical techniques to the study of whole cells capable of electron transfer to electrodes. Busalmen et al. detected signatures characterisic of *c*-type cytochromes at a *Geobacter* cell–electrode interface using surface-enhanced infrared absorption,[27] while Nakamura et al. were able to detect redox-dependent changes in the Soret-band characteristic of *c*-type cytochromes in *Shewanella* suspensions, using evanscent wave spectroscopy.[28]

These previous studies primarily examined concentrated cell suspensions for short periods of time. However, it is well known that biofilm growth requires disctrete attachment, biosynthesis, and secretion events to construct the external network of delicate proteins that transports electrons from cells.[18,29–33] Thus, the goal of this work was was to design a system able to support growth of metal-reducing bacteria on transparent conductive electrodes to link potential-dependent changes with real-time measurements of spectral signatures in an undamaged biofilm network (Figure 1).

Extensive physiological, proteomic, mRNA expression, and imaging data already exists describing *Geobacter* biofilm growth on graphitic carbon and gold electrodes. To investigate whether data from this well-understood model could be com-

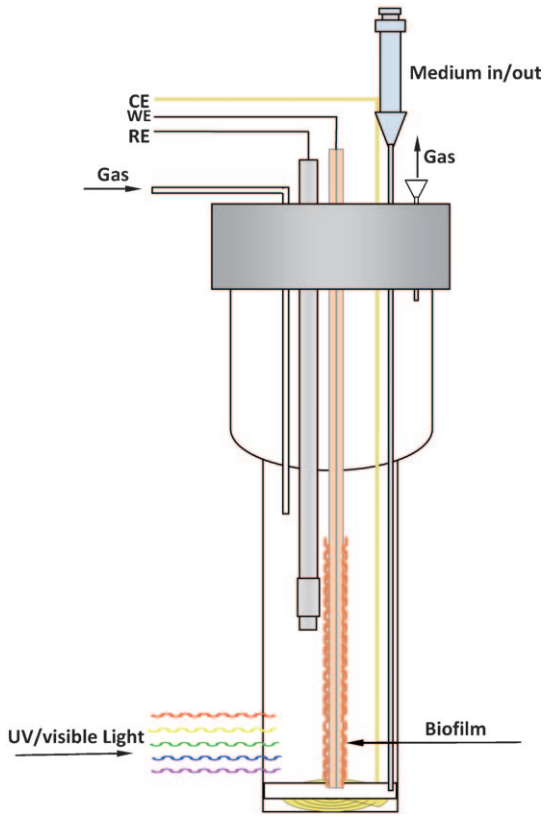

Figure 1. Diagram showing the anaerobic spectroelectrochemical reactor designed for this study. The use of a quartz chamber and a double-sided ITO-coated glass electrode maximized the optical signals. The reactor was maintained at 30 °C with magnetically driven agitation to allow simultaneous growth, electrochemistry, and spectral analysis (WE: working electrode; CE: counter electrode; RE: reference electrode).

[a] *Dr. Y. Liu, Dr. D. R. Bond*
BioTechnology Institute and Department of Microbiology
University of Minnesota, 140 Gortner Laboratory
1479 Gortner Ave, St. Paul MN 55108 (USA)
E-mail: dbond@umn.edu

[b] *Dr. H. Kim, Dr. R. R. Franklin*
Department of Electrical Engineering and Computer Science
University of Minnesota (USA)

Supporting information for this article is available on the WWW under http://dx.doi.org/10.1002/cphc.201100246.

pared to growth on indium tin oxide (ITO) surfaces, we placed electrodes coated with electroplated gold in the same reactor with ITO electrodes, and exposed both to a culture of *G. sulfurreducens* to simultaneously measure colonization rates and current densities.

While no toxicity or attachment issues were observed, the choice of high- versus low-resistance ITO films was found to exert a strong influence on the results. Example data comparing low-resistance ITO (sheet resistance of 30 Ω per square) and high-resistance ITO (100 Ω per square) with gold electrodes of identical geometric surface areas are shown in Figure 2.

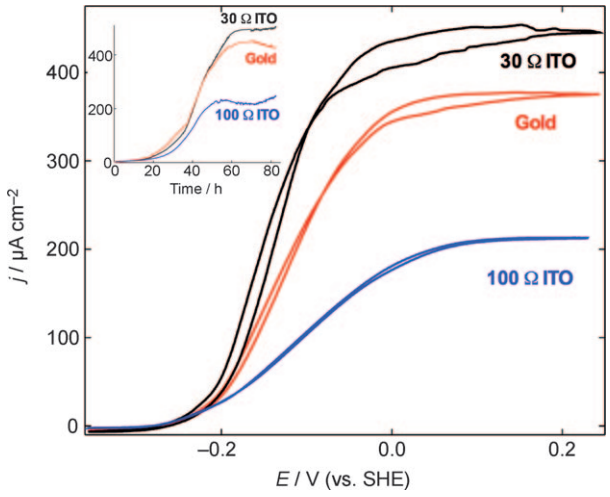

Figure 2. Cyclic voltammetry (1 mV s^{-1}) for *G. sulfurreducens* biofilms oxidizing acetate using identically sized 30 Ω (black), 100 Ω (blue) ITO, or electroplated gold electrodes (red). Inset: Chronoamperometry showing colonization of the surfaces. By including multiple electrodes in the same reactor, all electrodes were exposed to identical culture conditions for testing.

Screening of a range of electrode surfaces demonstrated that only low-resistance ITO electrodes supported rapid *Geobacter* attachment, produced identical growth rates, and repeatable current densities (440 μA cm^{-2} +/-25, $n=5$) seen with more commonly used gold and graphite[1] electrodes, and could be compared with previous studies.

Two techniques used to study bacterial redox proteins in communication with electrodes are slow-scan-rate voltammetry in the presence of electron donors (catalytic voltammetry), and scan-rate analysis in the absence of electron donors (single-turnover voltammetry). As shown in Figure 2, sigmoidal catalytic waves were obtained for both gold and ITO electrodes, with similar onset and midpoint potentials,[1,2] further illustrating the similarity between electron transfer to these materials when low-resistance ITO was used.

In the absence of electron donor, the number of detected redox species (Figure 3) and their apparent redox potentials were also similar to what has been reported with gold and graphite electrodes. Scan-rate analysis comparing ITO and gold-grown biofilms showed that the peak height increased proportional to the square root of the scan rate for both biofilms above scan rates of 1 mV s^{-1}. This relationship verified

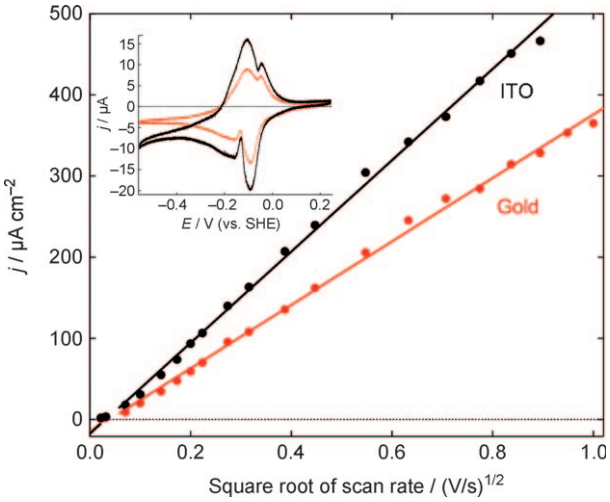

Figure 3. Single-turnover scan-rate analysis of donor-starved gold (red) and ITO (black) *G. sulfurreducens* biofilms, showing similar scan-rate dependence and semi-infinite kinetics above rates of 1 mV s^{-1}. Inset: non-baseline-subtracted single-turnover voltammogram (5 mV s^{-1}) showing similar potentials of main redox peaks regardless of the electrode material used.

that electron transfer through the biofilm above these scan rates did not follow thin-film kinetics, but rather behaved according to the semi-infinite diffusion behavior reported for electron transfer within *Geobacter* biofilms.[1,2,5,7,8] This behavior is common for systems in which the interfacial electron-transfer reaction is fast compared to the rate electrons are exchanged between redox species within a film, such as redox polymers.[34] Most importantly for this work, the kinetics of electron transfer through this film during single-turnover voltammetry was comparable, regardless of the electrode material chosen.

Imaging of biofilms grown for 140 h on low-resistance ITO using laser scanning confocal microscopy revealed uniform coverage of the electrodes, to a consistent thickness (averaging 30 μm) with no large pillar or mushroom-like structures, after the culture reaches a stable current density. Based on LIVE/DEAD staining to asses membrane integrity (see Figure S1 of the Supporting Information), ITO-grown films were dominated by live cells, even after multiple manipulations (starvation for cyclic voltammetry, recovery and growth in plateau phase for more than three days).

Peeling of the biofilm from the electrode was found in a small percentage of sites after rapid dehydration for scanning electron microscopy analysis, by omission of the critical point drying step (Figure 4, complete confocal images for comparison in the Supporting Information, Figure S1). Imaging within these fractured regions revealed a highly ordered layer of *Geobacter* cells, typically oriented along the long axis of the cells.

This series of comparisons demonstrated that 1) consistent biofilms with similar growth and electrochemical properties as those studied with gold or graphite could be grown on low-resistance ITO electrodes, and 2) these films were dominated by a uniform film of live cells that remained viable after starvation. These results supported the use of ITO in stirred quartz cuvettes for study of *Geobacter,* and showed that growth charac-

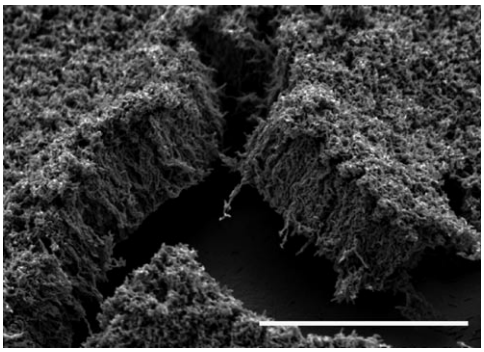

Figure 4. Scanning electron micrograph (scale bar = 50 μm) of a region of an ITO-grown biofilm intentionally cracked during dehydration, to reveal biofilm organization throughout the area. Cracking was not observed during normal dehydration and critical-point drying, but this manipulation could be used to reveal the thickness and interior architecture of the film.

teristics in our reactor could be compared with previous data using graphite or gold electrodes.

For spectral studies, biofilms were grown to the point of constant current density using acetate as the electron donor, and medium in the reactor was replaced with electrolyte lacking electron donor. Cells were starved for 24 h to deplete intracellular reserves, and the medium in the reactor was replaced a second time. To test if cells adherent to the reactor walls contributed to absorbance, spectral scans were collected with and without the ITO electrode in place. The contribution from wall-attached cells was always less than 1% of the total ($n = 4$) at this stage, showing that spectral signals were primarily derived from electrode-attached bacteria. As planktonic bacteria are released from growing biofilms, and reactors could accumulate wall growth over time, controls to monitor this potential pool of non-attached bacteria should always be included in longer-term experiments.

Figure 5 shows representative complete spectral scans from a mature (~30 μm thick, 96 h of growth) biofilm of *G. sulfurreducens*, depleted of electron donors. Biofilms were pre-equilibrated at the set potential for 10 min (see Figure 7 for more data related to time required for equilibration). Dominant spectral signatures were observed in the 410–418 nm Soret region, as well as the 552 nm α and 523 nm β-bands that are characteristic for low-spin *c*-type cytochromes.[35] Minor shoulders indicative of high-spin hemes, peaks characteristic of other heme species or His-Met coordination, peaks characteristic of multicopper proteins, or peaks attributible to known redox-active compounds were not obvious in this data, although the possibility remains that the *c*-type cytochrome spectral signatures overwhelmed minor peaks.

These spectral features responded immediately to changes in imposed voltage across a wide potential window. Complete reduction was observed below −0.35 V, and complete oxidation occured above +0.1 V, based on both characteristic wavelengths used to measure cytochrome redox state. In separate experiments, when biofilms oxidized at +0.2 V were exposed to air, no further increases in *c*-type cytochrome absorbance signatures were observed ($n = 3$), further demonstrating that

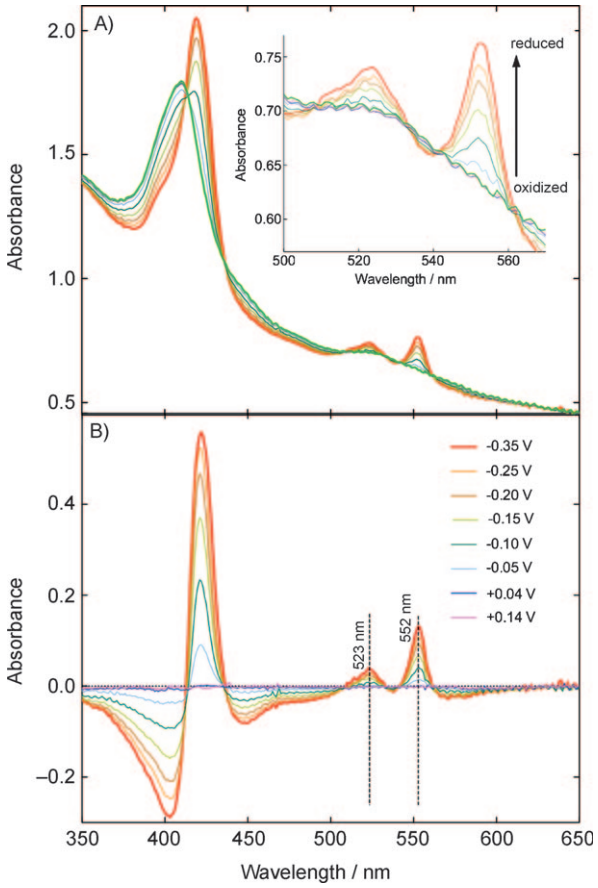

Figure 5. A) Spectral data from *G. sulfurreducens* biofilms grown on ITO electrodes, starved free of electron donors and washed to remove planktonic cells. Each scan was collected after the biofilm was poised at the potential indicated for 10 min. Data in (B) shows reduced minus oxidized spectra using biofilms at +0.240 V as the baseline. Wall growth in the cuvette was responsible for less thsan 1% of the spectral signals.

all cytochromes were accessible by the electrode in these studies.

Clear isosbestic points for each major peak could be identified and were used for estimation of the redox state of *c*-type cytochromes. When the change in either Soret (~410 nm) or α-band absorbance (552 nm) was plotted as a function of the applied potential, the predicted redox states of cytochromes in biofilms were identical. Films could be completely oxidized and reduced multiple times with no change in total absorbance or calculated redox status.

As these spectral scan experiments at poised potentials were highly repeatable, and either wavelength was able to produce identical readouts of redox status, this provided support for the use of a subset of wavelengths as indicators of baselines (isosbestic points), and redox status during linear sweep voltammetry. This allowed many measurements per second to be collected from each wavelength during voltammetry. The aim of these experiments was to measure the average redox status of all *c*-type cytochromes in the biofilm across a range of imposed redox potentials. To do this, it was first nessecary to prove that the scan rate did not affect the re-

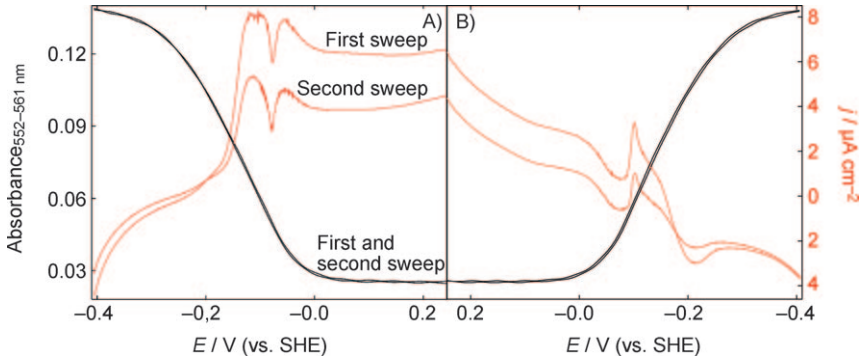

Figure 6. Raw data from slow-scan-rate linear-sweep voltammetry (0.1 mV s^{-1}) for *G. sulfurreducens* biofilms (red traces) showing two successive anodic sweeps (A) and cathodic sweeps (B). Note the reversal of the potential scale in (B). The black traces show the raw absorbance difference (552 nm–561 nm) for both sweeps. Minor differences in voltammetry could be observed due to residual catalytic activity, but the spectral signals were identical between the sweeps, in both directions.

sults, and that the redox status did not depend upon the sweep direction or the number of cycles.

Figure 6 shows raw voltammetry data (in red) from two linear sweep cycles at a scan rate ten times slower than what is typically used with this organism (0.1 mV s^{-1}). Figure 6 also shows raw absorbance changes (in black) due to cytochrome oxidation for each sweep. The major finding of these repeated slow-scan-rate experiments was that the spectral data obtained in both the anodic and cathodic directions during all replicates was identical when 0.1 mV s^{-1} scan rates were used. Thus, this scan rate is slow enough to allow all cytochromes in the film to equilibrate with the set potential of the electrode and reveal their redox state, independent of kinetic effects.

A second variable investigated was the effect of increasing the scan rate. Biofilms subjected to linear-sweep voltammetry at 0.2 mV s^{-1} showed an identical relationship to what is shown in Figure 6. However, raising the scan rate to 1 mV s^{-1} began to reveal hysteresis. Data comparing 0.1 mV s^{-1} and 1 mV s^{-1}, as well as data from electrodes held for ten minutes at each potential, are overlaid in Figure 7B. These comparisons provide a redox titation for the complete suite of electrode-accesible cytochromes within intact *G. sulfurreducens* biofilms and show that even at scan rates of 1 mV s^{-1}, some cytochromes within the biofilm do not have time to adjust to the imposed potential.

The fact that the spectral data from the forward and reverse sweeps lagged behind voltage changes at scan rates greater than 1 mV s^{-1} agreed with the results of electrochemical analysis, which measured semi-infinite diffusional kinetics above these scan rates (Figure 3). On timescales slower than 1 mV s^{-1}, the rate of electron transfer within the film was rapid enough to prevent gradients from forming, and all cytochromes within the film equilibrated with the electrode. As the scan rate exceeded the time needed for electrons to travel from within the biofilm to the electrode, the redox state of some cytochromes lagged behind the imposed potential, causing parts of the curve in Figure 7B to shift to more positive potentials during the anodic sweep and more negative potentials during the cathodic sweep. At 1 mV s^{-1}, this hysteresis was subtle, but was most noticeable in the higher potential window, and was seen in all experiments. This kinetic deviation will be highly useful in future studies, as it indicates that spectroelectrochemical analysis may be able to resolve differences between individual cytochrome oxidation rates in the biofilm.

When the total Coulombs of charge collected during baseline-subtracted voltammograms were intergrated, it was possible to calculate the potentials at which the film discharged 25, 50, and 75% of its electrons (averaged for forward and reverse sweeps). These measurements agreed within 10 mV of the same estimates calculated from *c*-type cytochrome absorbance. In other words, when 25% of the electrons stored within the biofilm were collected by the potentiostat, a 25% drop in the *c*-type cytochrome signal was measured. This agreement between electron-discharge data and spectral data provides independent evidence that the overwhelming majority of electrons stored within these *Geobacter* biofilms at physiological potentials reside in *c*-type cytochromes and not in other redox-active proteins or molecules. Such observations support the concept of the *c*-type cytochrome pool as the primary reservoir for electron storage by *Geobacter*.[36,37] These calculations were performed within a potential range spanning the known range of metal-oxide electron acceptors, where water, proteins, and DNA are stable (−0.4 to +0.4 V). While the use of higher[27] or lower voltages may reveal additional redox acitivty or electron storage, it would need to be established if such events were damaging to the cell, and if they were equally reversible.

This data reveals many interesting features of the *Geobacter* cytochrome network, especially when considered in the context of potentials required to drive anodic electron transfer out of the bacterium. First, nearly 35% of cellular cytochromes are oxidized within the lower −0.4 to −0.22 V window (Figure 7B), yet catalytic voltammetry has never shown significant anodic current when electrodes are poised in this range (Figure 3). This suggests that electron transfer via these cytochromes is not what controls electron transfer out of the cell. Second, this redox window is not symmetrical, dropping off steeply after −0.15 V to become fully oxidized by 0 V (Figure 7C), indicating a lack of cytochromes with potentials above this range.

As we designed these experiments to create the same conditions previously used to obtain biochemical and transcriptional information from *G. sulfurreducens*, it is possible to directly compare the redox behavior in biofilms with redox potentials of outer-surface cytochromes known to be expressed under these growth conditions by *Geobacter*. The macroscopic redox potentials of four multiheme cytochromes abundant in electrode-grown biofilms of *G. sulfurreducens* have been re-

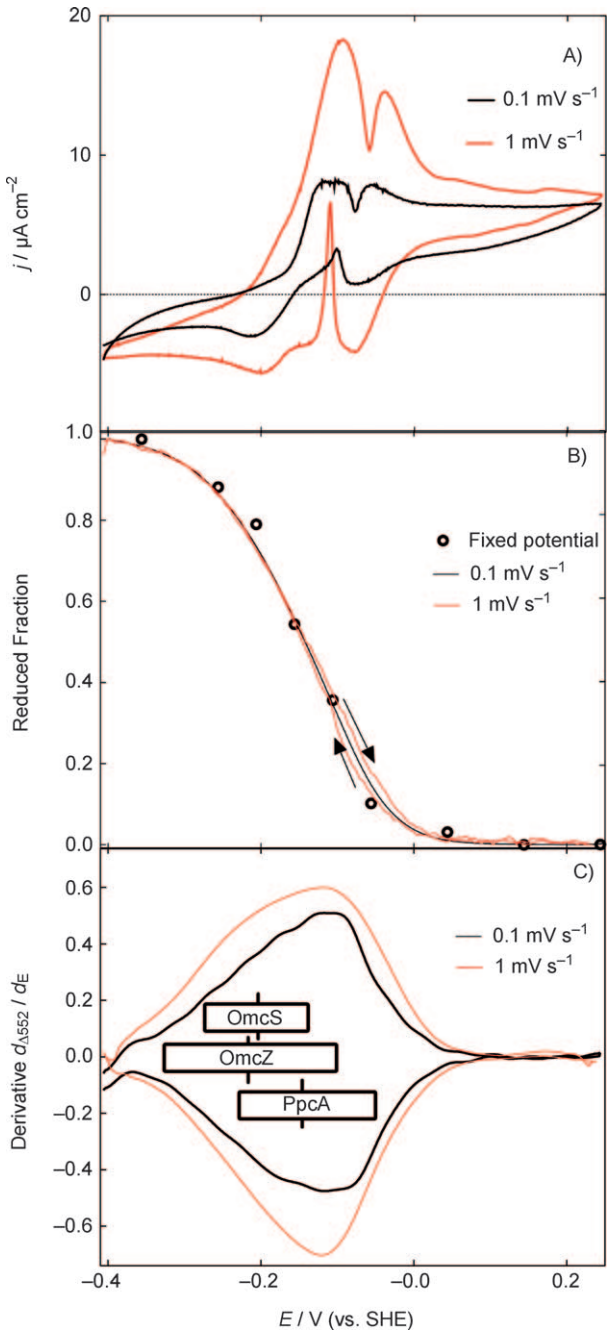

Figure 7. Correlation between potential and oxidation state of biofilm cytochromes in the absence of an electron donor. A) Cyclic voltammetry at 0.1 mV s^{-1} (black) and 1 mV s^{-1} (red), non-baseline-subtracted. B) Fraction of *c*-type cytochromes reduced in the biofilm as a function of the potential. The round symbols are from poising the biofilm for 10 min before each determination; the black lines show anodic and cathodic 0.1 mV s^{-1} sweeps; and the red lines show the anodic and cathodic 1 mV s^{-1} sweeps. C) Derivative of (B), with the bars representing windows spanning 90% oxidation and reduction for three highly abundant multiheme cytochromes in *Geobacter*.

ported. The octoheme cytochrome OmcZ has a broad potential window spanning from −420 to −60 mV, and centered at −220 mV,[16] while the hexaheme cytochrome OmcS is oxidized over a range of −360 to −40 mV, centered at −212 mV.[19] OmcZ is found loosely attached to the outer-surface matrix, while OmcS has been found to coat pili; thus, these proteins would be predicted to be farthest from the membrane and most accesible to the electrodes.[16,18] The little data available for the dodecaheme cytochrome OmcB, which is closely attached to the outer membrane, suggests an equally broad window centered around a macroscopic potential of −190 mV.[38]

Interestingly, these low-potential ranges reported for proteins found beyond the cell membrane agree with the large amount of cytochrome we detect between −0.4 V and −0.1 V. The broad shape of the low-potential window is also in agreement with the wide redox windows of OmcB, OmcS, and OmcZ. As the extinction coefficients for multiheme cytochromes (at 410 nm) have been reported to vary from at least 424400 to 1670000 M^{-1} cm^{-1},[16,19,39] it is not possible to use spectral data to estimate the amounts of cytochrome detected by spectroscopy, but integration of coulombic data and the nonsymmetrical nature of the redox curve shows that lower potential cytochromes are a major component of the conductive biofilm.

The triheme cytochrome PpcA, which is highly abundant in the periplasm of *G. sulfurreducens*, is the likely reservoir of electrons destined for the outer surface.[14,40] Its macroscopic redox potential is centered at −146 mV, although a cycle of protonation and deprotonation alters the microscopic redox potential of heme III to higher values (−123 mV) during oxidiation, and lower values (−185 mV) during reduction.[41,42] This potential window is consistent with the sharp transition seen in biofilm oxidation state at higher potentials, in the −150 mV range.

This observation that extracellular cytochromes have lower potentials than periplasmic cytochromes raises interesting questions unique to the *Geobacter* electron-transfer system. As periplasmic PpcA cannot be in contact with the electrode, it must rely upon outer-surface proteins to mediate transfer of electrons outward. The fact that the outer-surface cytochromes OmcB, OmcS, and OmcZ have lower formal potentials than PpcA, yet are among the best candidates to serve as mediators of electron transfer, is the opposite of how typical electron-transfer chains are designed. A hypothesis for this arrangement is that cells evolved to guarantee that their outer surface network is always in an oxidized state, even when low-potential acceptors are available, so they may always act as an acceptor for the periplasmic pool.

Such an arrangement seems counterintuitive, but is feasible if the electron-transfer rate constant for interfacial transfer between the cytochrome pool and the electrode surface is very fast, allowing this bound mediator pool to rapidly equilibrate with the electrode. A similar model was proposed recently in electrochemical simulations of *Geobacter* biofilms.[4] One prediction made by this hypothesis is that the periplasmic pool, being 'upstream' of this lower potential between-cell pool, would be slower to respond to changes in electrode potential. This is exactly what is seen as the scan rate is increased: while the response at lower potentials remains similar, the spectral changes in the −150 mV window lag behind. A second prediction from this arrangement would be that the redox status of the periplasmic cytochrome would 'gate' electron flow to the

exterior, which would explain the −150 mV midpoint potential of catalytic cyclic voltammetry data.

As this same spectral methodology can be used to analyze biofilms under catalytic condidions, it will be of interest what the sequence of oxidation events is at faster scan rates, especially when these cytochromes are engaged in the active transport of electrons. By combining this with mutant analysis using cells expressing different levels of these cytochromes, studies may be able to resolve how *Geobacter* creates a multiprotein electron-transfer network that rivals the current densities of the best-known chemically synthesized redox hydrogels.

Experimental Section

Electrochemistry and UV/Vis Spectroscopy: Chronoamperometry (CA) was performed on a 16-channel potentiostat and cyclic voltammetry (CV) was conducted using a Gamry PCI4 Femtostat. Gold electrodes or ITO electrodes were used as working electrodes. Pt wires and calomel reference electrodes consisting of mercury/mercurous chloride and saturated potassium chloride (saturated calomel reference, SCE, 0.244 V vs. the standard hydrogen electrode, SHE) were used as counter electrode and reference electrode, respectively. All potentials are versus SHE. The scan-rate analysis was done using starved cells in a non-turnover state. A SpectraMaxPlus384 (Molecular Devices, California, USA) was used to measure the UV/Vis spectrum using a quartz cuvette of 10 mm path length (Starna Cells, Atascadero, CA, USA) with a custom-joint to a top that could be sealed with a butyl stopper to exclude oxygen (Figure 1). All experiments were conducted at 30 °C.

Bacterial Strain, Culture Media, Biofilm Growth, ITO Glass, and Gold Electrode Preparation: G. sulfurreducens strain PCA (ATCC51573) was subcultured in our lab at 30 °C using a vitamin-free anaerobic medium, as previously described.[1,2] Acetate was provided as an electron donor at 30 mM. All media were adjusted to pH 6.8 prior to the addition of 2 g L^{-1} $NaHCO_3$ and were flushed with oxygen-free N_2–CO_2 (80:20 [vol/vol]) prior to sealing with butyl rubber stoppers. All experiments were initiated by inoculating with 40% (vol/vol) of cells within 3 h of reaching maximum optical density (OD > 0.6) in the medium described, with 40 mM fumarate as the electron acceptor. ITO-coated glass was ordered from Bayview Optics (Maine) with a working area of 1 cm^2, and was cleaned in acetone and deionized water, respectively. Gold electrodes were made by electroplating gold onto a silicon wafer with the same working surface area, and were cleaned with 1 M nitric acid, ethanol, and then scanned within the potential range of 0.244 to 1.744 V in 0.5 M H_2SO_4 until a voltammogram characteristic of a gold electrode was established.

Confocal Microscopy and Scanning Electron Microscopy (SEM) Analysis: Biofilms on electrodes were stained with the LIVE/DEAD Baclight bacterial viability kit (Invitrogen, Carlsbad, CA) and was viewed with a Nikon Eclipse C1 confocal microscope using 488 nm and 561 nm filters. A S3500N SEM (Hitachi, Japan) was also used to image the biofilms. After the biofilms were fixed in 2.5% glutaraldehyde overnight, they were immersed in 1% osmium tetroxide, washed, and then dehydrated in 25, 50, 75, 95, and 100% ethanol. After critical point drying, the samples were sputtered with gold.[1]

[1] *As this article went to press, a similar approach was reported in Electrochemica Acta by Jain et al. (DOI: 10.1016/j.electacta.2011.02.073)*

Acknowledgements

This work was supported by the National Science Foundation (ECS 0702200) and the Office of Naval Research (NM000140810162)

Keywords: bacteria · biofilms · cytochromes · electrochemistry · spectroelectrochemistry

[1] E. Marsili, J. Sun, D. R. Bond, *Electroanalysis* **2010**, *22*, 865 – 874.
[2] E. Marsili, J. B. Rollefson, D. B. Baron, R. M. Hozalski, D. R. Bond, *Appl. Environ. Microbiol.* **2008**, *74*, 7329 – 7337.
[3] G. Reguera, K. P. Nevin, J. S. Nicoll, S. F. Covalla, T. L. Woodard, D. R. Lovley, *Appl. Environ. Microbiol.* **2006**, *72*, 7345 – 7348.
[4] S. M. Strycharz, A. P. Malanoski, R. M. Snider, H. Yi, D. R. Lovley, L. M. Tender, *Energy Environ. Sci.* **2011**, *4*, 896 – 913.
[5] K. P. Katuri, P. Kavanagh, S. Rengaraj, D. Leech, *Chem. Commun.* **2010**, *46*, 4758 – 4760.
[6] A. Heller, *Phys. Chem. Chem. Phys.* **2004**, *6*, 209 – 216.
[7] H. Richter, K. P. Nevin, H. F. Jia, D. A. Lowy, D. R. Lovley, L. M. Tender, *Energy Environ. Sci.* **2009**, *2*, 506 – 516.
[8] K. Fricke, F. Harnisch, U. Schröder, *Energy Environ. Sci.* **2008**, *1*, 144 – 147.
[9] D. B. Baron, E. Labelle, D. Coursolle, J. A. Gralnick, D. R. Bond, *J. Biol. Chem.* **2009**, *284*, 28865 – 28873.
[10] B. A. Methe, K. E. Nelson, J. A. Eisen, I. T. Paulsen, W. Nelson, J. F. Heidelberg, D. Wu, M. Wu, N. Ward, M. J. Beanan, R. J. Dodson, R. Madupu, L. M. Brinkac, S. C. Daugherty, R. T. DeBoy, A. S. Durkin, M. Gwinn, J. F. Kolonay, S. A. Sullivan, D. H. Haft, J. Selengut, T. M. Davidsen, N. Zafar, O. White, B. Tran, C. Romero, H. A. Forberger, J. Weidman, H. Khouri, T. V. Feldblyum, T. R. Utterback, Van S. E. Aken, D. R. Lovley, C. M. Fraser, *Science* **2003**, *302*, 1967 – 1969.
[11] J. E. Butler, N. D. Young, D. R. Lovley, *BMC Genomics* **2010**, *11*, 40.
[12] Y. Qiu, B.-K. Cho, Y. S. Park, D. Lovley, B. Palsson, K. Zengler, *Genome Res.* **2010**, *20*, 1304.
[13] M. Aklujkar, J. Krushkal, G. DiBartolo, A. Lapidus, M. L. Land, D. R. Lovley, *BMC Microbiol.* **2009**, *9*, 109.
[14] J. R. Lloyd, C. Leang, Hodges A. L. Myerson, M. V. Coppi, S. Cuifo, B. Methe, S. J. Sandler, D. R. Lovley, *Biochem. J.* **2003**, *369*, 153 – 161.
[15] X. Qian, G. Reguera, T. Mester, D. R. Lovley, *FEMS Microbiol. Lett.* **2007**, *277*, 21 – 27.
[16] K. Inoue, X. Qian, L. Morgado, B.-C. Kim, T. Mester, M. Izallalen, C. A. Salgueiro, D. R. Lovley, *Appl. Environ. Microbiol.* **2010**, *76*, 3999 – 4007.
[17] T. Mehta, S. E. Childers, R. Glaven, D. R. Lovley, T. Mester, *Microbiology* **2006**, *152*, 2257 – 2264.
[18] C. Leang, X. Qian, T. Mester, D. R. Lovley, *Appl. Environ. Microbiol.* **2010**, *76*, 4080 – 4084.
[19] X. Qian, T. Mester, L. Morgado, T. Arakawa, M. L. Sharma, K. Inoue, C. Joseph, C. A. Salgueiro, M. J. Maroney, D. R. Lovley, *Biochim. Biophys. Acta* **2011**, *1807*, 404 – 412.
[20] C. Leang, M. V. Coppi, D. R. Lovley, *J. Bacteriol.* **2003**, *185*, 2096 – 2103.
[21] B. C. Kim, C. Leang, Y. H. Ding, R. H. Glaven, M. V. Coppi, D. R. Lovley, *J. Bacteriol.* **2005**, *187*, 4505 – 4513.
[22] T. Mehta, M. V. Coppi, S. E. Childers, D. R. Lovley, *Appl. Environ. Microbiol.* **2005**, *71*, 8634 – 8641.
[23] J. E. Butler, F. Kaufmann, M. V. Coppi, C. Núñez, D. R. Lovley, *J. Bacteriol.* **2004**, *186*, 4042 – 4045.
[24] P.-L. Tremblay, Z. M. Summers, R. H. Glaven, K. P. Nevin, K. Zengler, C. L. Barrett, Y. Qiu, B. O. Palsson, D. R. Lovley, *Environ. Microbiol.* **2011**, *13*, 13 – 23.
[25] S. J. Marritt, G. L. Kemp, L. Xiaoe, J. R. Durrant, M. R. Cheesman, J. N. Butt, *J. Am. Chem. Soc.* **2008**, *130*, 8588 – 8592.
[26] Y. Astuti, E. Topoglidis, G. Gilardi, J. R. Durrant, *Bioelectrochemistry* **2004**, *63*, 55 – 59.
[27] J. P. Busalmen, A. Esteve-Nuñez, A. Berná, J. M. Feliu, *Bioelectrochemistry* **2010**, *78*, 25 – 29.
[28] R. Nakamura, K. Ishii, K. Hashimoto, *Angew. Chem.* **2009**, *121*, 1634 – 1636; *Angew. Chem. Int. Ed.* **2009**, *48*, 1606 – 1608.

[29] K. P. Nevin, B. C. Kim, R. H. Glaven, J. P. Johnson, T. L. Woodard, B. A. Methe, R. J. Didonato, S. F. Covalla, A. E. Franks, A. Liu, D. R. Lovley, *PLoS One* **2009**, *4*, e5628.
[30] A. E. Franks, K. P. Nevin, H. F. Jia, M. Izallalen, T. L. Woodard, D. R. Lovley, *Energy Environ. Sci.* **2009**, *2*, 113 – 119.
[31] K. Inoue, C. Leang, A. Franks, T. Woodard, K. Nevin, D. R. Lovley, *Env. Microbiol. Reports*, **2010**, DOI: 10.1111/j.1758-2229.2010.00210.x.
[32] J. B. Rollefson, C. S. Stephen, M. Tien, D. R. Bond, *J. Bacteriol.* **2011**, *193*, 1023 – 1033.
[33] A. E. Franks, K. P. Nevin, R. H. Glaven, D. R. Lovley, *ISME J.* **2010**, *4*, 509 – 519.
[34] R. J. Forster, J. G. Vos, *Electrochim. Acta* **1992**, *37*, 159 – 167.
[35] J. E. Falk, *Porphyrins and Metalloporphyrins, Vol. 2*, Elsevier Publishing, Amsterdam, **1964**.
[36] A. Esteve-Núñez, J. Sosnik, P. Visconti, D. R. Lovley, *Environ. Microbiol.* **2008**, *10*, 497 – 505.
[37] J. Zhao, Y. Fang, T. D. Scheibe, D. R. Lovley, R. Mahadevan, *J. Contam. Hydrol.* **2010**, *112*, 30 – 44.
[38] T. S. Magnuson, N. Isoyama, A. L. Hodges-Myerson, G. Davidson, M. J. Maroney, G. G. Geesey, D. R. Lovley, *Biochem. J.* **2001**, *359*, 147 – 152.
[39] D. E. Ross, S. L. Brantley, M. Tien, *Appl. Environ. Microbiol.* **2009**, *75*, 5218 – 5226.
[40] Y. H. R. Ding, K. K. Hixson, C. S. Giometti, A. Stanley, A. Esteve-Nunez, T. Khare, S. L. Tollaksen, W. H. Zhu, J. N. Adkins, M. S. Lipton, R. D. Smith, T. Mester, D. R. Lovley, *BBA-Proteins and Proteomics* **2006**, *1764*, 1198 – 1206.
[41] M. Pessanha, L. Morgado, R. O. Louro, Y. Y. Londer, P. R. Pokkuluri, M. Schiffer, C. A. Salgueiro, *Biochemistry* **2006**, *45*, 13910 – 13917.
[42] L. Morgado, M. Bruix, M. Pessanha, Y. Y. Londer, C. A. Salgueiro, *Biophys. J.* **2010**, *99*, 293 – 301.

Received: March 29, 2011
Published online on ■■ ■■, 0000

COMMUNICATIONS

*Y. Liu, H. Kim, R. R. Franklin, D. R. Bond**

■■ – ■■

Linking Spectral and Electrochemical Analysis to Monitor *c*-type Cytochrome Redox Status in Living *Geobacter sulfurreducens* Biofilms

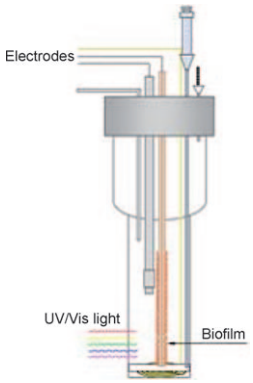

Biofilm synesthesia: A simultaneous spectral and electrochemical analysis reveals the redox status of cytochromes within living electroactive biofilms of *Geobacter*. The results confirm that the primary electron reservoirs within these biofilms are *c*-type cytochromes and suggest which cytochromes act as kinetic bottlenecks to electron transfer.

CHEMPHYSCHEM

Supporting Information

Linking Spectral and Electrochemical Analysis to Monitor *c*-type Cytochrome Redox Status in Living *Geobacter sulfurreducens* Biofilms

Ying Liu,[a] Hoseang Kim,[b] Rhonda R. Franklin,[b] and Daniel R. Bond*[a]

cphc_201100246_sm_miscellaneous_information.pdf

Supplementary Figure 1

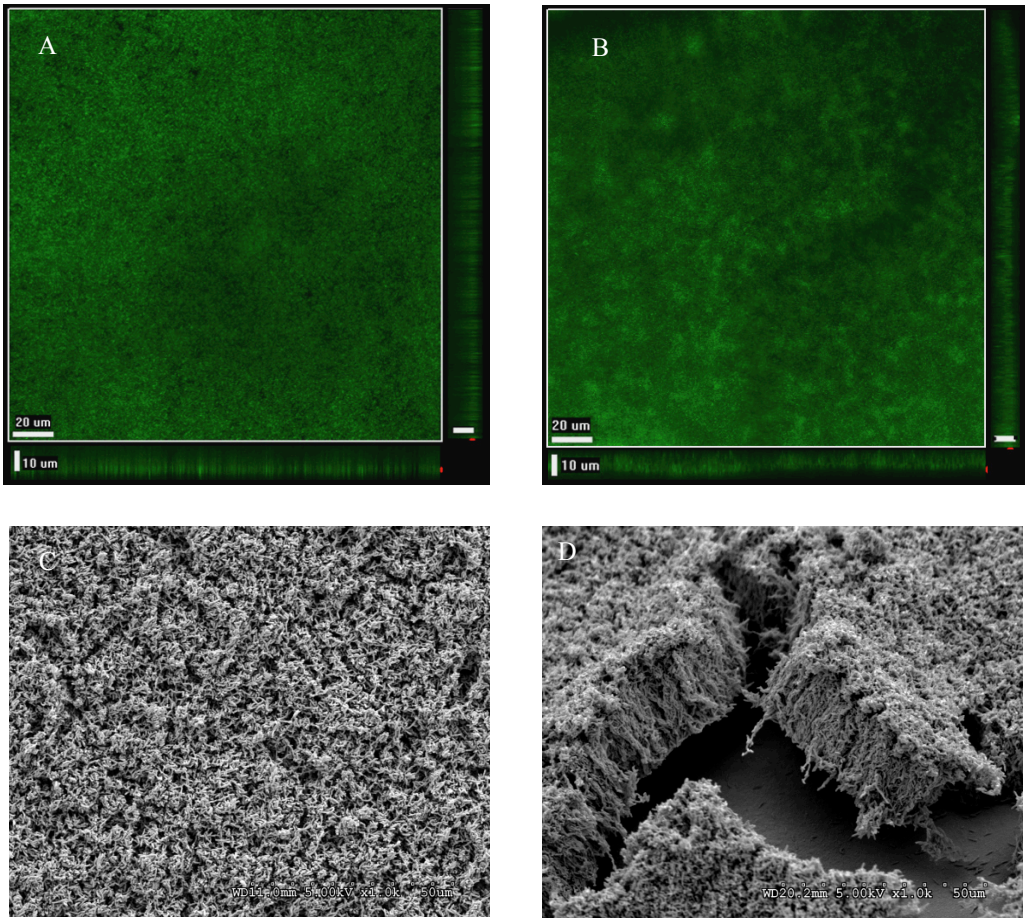

Supplementary Figure 1; Comparison of confocal (A, C) and scanning electron microscopy (B, D) images of *G. sulfurreducens* biofilms cultivated for 96 h on gold or ITO electrodes. Confcoal images are stained with Live/Dead (Green/Red) viability stain, revealing intact cells as green and putatively dead or damaged cells as red. Release of biofilms from ITO was occasionally observed when films were rapidly dehydrated, suggesting weaker adhesion to ITO surfaces.